Microchimica Acta (2019) 186: 832
https://doi.org/10.1007/s00604-019-3916-5

ORIGINAL PAPER

Binary magnetic metal-organic frameworks composites: a promising affinity probe for highly selective and rapid enrichment of mono- and multi-phosphopeptides

Baichun Wang[1] · Bin Liu[1] · Yinghua Yan[1] · Keqi Tang[1] · Chuan-Fan Ding[1]

Received: 31 May 2019 / Accepted: 11 October 2019 / Published online: 22 November 2019

Abstract

A binary magnetic metal-organic framework (MOF)-functionalized material (magG@PDA@Ni-MOF@Fe-MOF) was prepared through grafting Ni-MOF and Fe-MOF on magnetic (Fe_3O_4) graphene with polydopamine (PDA) as a middle layer. Compared with single MOFs functionalized materials (magG@PDA@Ni-MOF and magG@PDA@Fe-MOF) under the same conditions, magG@PDA@Ni-MOF@Fe-MOF not only displays lower detection limits (4 fmol) and selectivity (1:1000), but also has better enrichment efficiency for both multi- and monophosphopeptides. Other than this, magG@PDA@Ni-MOF@Fe-MOF exhibits fine reusability (five cycles) and rapid enrichment property (1 min), and 24 phosphopeptides were detected when it was applied to the analysis of human saliva.

Keywords Metal-organic frameworks (MOFs) · MagG@PDA@Ni-MOF@Fe-MOF · Immobilized metal ion affinity chromatography (IMAC) · MALDI-TOF mass spectrometry · Phosphopeptides

Introduction

Phosphorylated proteins play a significant role in controlling cellular functions such as metabolism, genetic expression [1, 2, 3], and in site-specific phosphorylation. In addition, some phosphorylated proteins act as molecular switches to inhibit or activate protein activity [4]. Furthermore, some serious disease such as cancer have already been proved to have something to do with them [5]. So the research of protein phosphorylation is of great importance, and the accurate identification of phosphorylation sites has become the precondition [6].

Based on the features of high accuracy, high throughput, easy operation and fast detection, mass spectrometry (MS) has become a common tool to satisfy the demand of determining phosphopeptides [7]. However, phosphopeptides were hard to analyse directly using mass spectrometry, which was ascribed to the interference of nonphosphopeptides and the insufficient ionization efficiency of phosphopeptides [8]. Hence, how efficiently enrich low-abundance peptides and simultaneously preclude high-abundance peptides have become an urgent issue to be resolved [9].

Plentiful strategies have been raised to fulfill the target of the enrichment of phosphopeptides, such as immobilized metal ion affinity chromatography (IMAC) [10], molecular imprinting technology [11], strong anion exchange chromatography (SAX) [12], amino functionalization [13], and metal oxide affinity chromatography (MOAC) [14]. Among the above strategies, MOAC and IMAC, with the strong electrostatic action between phosphopeptide/phosphoprotein and metal oxides/metal ions, have become the widespread method [15]. Nowadays, a heated trend about exploiting various chelates to graft metal oxides/metal ions onto carrier stuff to prepare functional materials for capturing phosphopeptides is under way [16]. For example, Deng group prepared Fe_3O_4@mTiO_2-MSA by coating a layer of

Electronic supplementary material The online version of this article (https://doi.org/10.1007/s00604-019-3916-5) contains supplementary material, which is available to authorized users.

✉ Yinghua Yan
yanyinghua@nbu.edu.cn

✉ Keqi Tang
tangkeqi@nbu.edu.cn

[1] School of Materials Science and Chemical Engineering, Institute of Mass Spectrometry, Ningbo University, Ningbo 315211, China

mesoporous titania on the surface of the magnetic ball [17]. These nanospheres with large specific surface area achieved good results in the enrichment of phosphopeptides and had an extremely low detection limit. Xie group utilized six phosphate groups of phytic acid to anchor a large amount of Ti(IV) ions on the magnetic sphere to synthesize Ti-PA-MNPs [18]. And the material had captured 2145 phosphopeptides from tryptic digest of a rat liver lysate, showing the strong application potential in the enrichment of phosphopeptides from biological samples. Nevertheless, these materials cannot be used to clearly distinguish multi- and monophosphopeptides. Thus, Deng group combined the features of IMAC and MOAC to synthesize a novel probe T2M for enrichment of phosphopeptides [19]. This probe integrated titania and titanium ions on the surface of the magnetic sphere, thereby realizing the global phosphopeptides enrichment. However, it took a mountain of steps and time to modify metal ions and metal oxides onto the same substrate, so it was still a need to develop novel materials that were easier to prepare to meet global phosphopeptide enrichment.

Metal-organic frameworks (MOFs), a new porous material, utilizes organic ligands and metal ions as building units and through ordered construct to constitute a magical legoland [20, 21]. With the unique performance of stupendous surface area, numerous surface active sites [22], high porosity [23], MOFs is widely applied in gas separation [24], catalysis [25] and sensing of small molecules [26]. It takes for granted that MOFs spurs great enthusiasm of researchers. Known literature revealed, an IMAC bead can obtain brilliant phosphopeptides capture efficiency with stupendous surface area, plentiful binding sites, a porous structure, which exactly is the superiority of MOFs [27]. Therefore, based on the pore structure and a large number of active metal centers of MOFs, it has great potential as a novel IMAC matrix. Relevant investigation pointed out, different metal ions have different biases for multi- and monophosphopeptides [28]. If two metal ions with different biases were combined, a complementary enrichment effect is obtained. For example, compared with single IMAC (Fe(III), Ga(III)), the Ga(III)-Fe(III)-IMAC tactics can obtain several times phosphoproteomic coverage [29]. Thus, it is foreseeable that preparing a binary MOFs material which can be easily synthesized can achieve good results in the enrichment of phosphopeptides and achieve global phosphopeptides enrichment, which is also a good choice for the study of phosphopeptidomics research.

Herein, a new composite material was synthesized by firstly depositing Ni-MOF on magG@PDA through ultrasonication to form magG@PDA@Ni-MOF [30], and then Fe-MOF was deposited on Ni-MOF in the same method to form magG@PDA@Ni-MOF@Fe-MOF. Graphene, since its introduction, had acquired a great attention and became an excellent carrier material due to the low manufacture costs and high specific surface area [31]. With the feature of paramagnetic, magnetic graphene allowed material to quickly detach from sample solution, facilitating experimental operations and improving accuracy [32]. And modifying polydopamine (PDA) onto material had increased the hydrophilicity of magnetic graphene [33]. Moreover, PDA contained numerous functional groups that can be utilized as the anchors of transition metal ions, thereby further enabling the synthesis of various kinds of composite materials [34]. Based on the electrostatic action with phosphopeptides, the binary MOF-functionalized material can carry out the aim of the enrichment of phosphopeptides. Therefore, combining all the merits mentioned above, the material what we expected was designed. In addition, a study comparing magG@PDA@Ni-MOF@Fe-MOF with single metal ion functionalized material (magG@PDA@Ni-MOF and magG@PDA@Fe-MOF) under the same conditions had been performed.

Experimental section

Reagents and chemicals

$NiCl_2 \cdot 6H_2O$, $FeCl_3 \cdot 6H_2O$, 1,4-dicarboxybenzene (1,4-BDC), and hydrochloric acid (HCl) were purchased from J&K Chemical Ltd. Dopamine hydrochloride, triethylamine (TEA), sodium acetate anhydrous, and ethanol were purchased from Aladdin Chemistry. N,N-Dimethylformamide (DMF), dithiothreitol (DTT), bovine β-casein, trypsin, indoacetamide (IAA), acetonitrile (ACN), bovine serum albumin (BSA), ammonia aqueous solution, ammonium bicarbonate (NH_4HCO_3) were purchased from Sigma Aldrich. Concentrated nitric acid, trisodium citrate, trifluoroacetic acid (TFA), polyethylene glycol, and sodium hydroxide were purchased from Shanghai Chemical Corporation. Human saliva and human serum were collected from the students of Ningbo University.

Apparatus

Philips XL30 (Netherlands) was utilized to obtain the SEM (scanning electron microscopy) image and EDX (energy dispersive X-rayspectroscopy) analysis of magG@PDA@Ni-MOF@Fe-MOF. Zetasizer (Nano Series, UK) was utilized to characterize the zeta potential of magG@PDA@Ni-MOF@Fe-MOF. JEOL 2011 microscope (Japan) was utilized to acquire the TEM (transmission electron microscopy) image of magG@PDA@Ni-MOF@Fe-MOF. Deionized water was got through using Milli-Q IQ7000. Fourier spectrophotometer (Nicolet 6700, USA)

was utilized to obtain the FT-IR (Fourier transform infrared Spectroscopy) spectra of magG@PDA@Ni-MOF@Fe-MOF.

Synthesis of magG@PDA@Ni-MOF

Firstly, magG@PDA (110 mg) was evenly dispersed by ultrasound in a mixed solution of deionized water (2 mL), ethanol (2 mL), and DMF (30 mL), followed by the addition of $NiCl_2 \cdot 6H_2O$ (180 mg) and 1,4-BDC (125 mg) into the above solution. Then, TEA (1 mL) was quickly inject into. Next, a uniform colloidal suspension was prepared via stirring the mixture for 10 min at room temperature. Subsequently, the suspension was sealed and ultrasonicated for 8 h. Last, through magnetic-separation techniques, magG@PDA@Ni-MOF we gained was washed with DMF (30 mL) and ethanol (30 mL) for three times each, then dry at 50 °C.

Synthesis of magG@PDA@Ni-MOF@Fe-MOF

In the first place, a solution was formed by adding 2 mL of deionized water and 2 mL of ethanol into 30 mL of DMF. Next, magG@PDA@Ni-MOF (70 mg) was evenly dispersed by ultrasound in the above solution to obtain a homogenous suspension. Then, sealed the homogenous suspension and ultrasonicated it for 3 h at room temperature. Subsequently, after adding 12 mg of $FeCl_3$, 60 mg of 1,4-BDC, and 1 mL of TEA, the mixture solution we gained was further ultrasonicated for 8 h. Last, through magnetic-separation techniques, magG@PDA@Ni-MOF@Fe-MOF was washed with DMF (30 mL) and ethanol (30 mL) for three times each, then dry at 50 °C.

Synthesis of magG@PDA@Fe-MOF

Firstly, it was mixed 2 mL of deionized water, 2 mL of ethanol and 30 mL of DMF to form a mixed solution. Next, magG@PDA (70 mg), $FeCl_3$ (12 mg), 1,4-BDC (60 mg) and TEA (1 mL) was added into the above solution. Then, sealed and ultrasonicated the solution for 8 h to obtain magG@PDA@Fe-MOF, which was further washed with DMF (30 mL) and ethanol (30 mL) for three times each, and dry at 50 °C.

Preparation of samples

Firstly, the 0.2% TFA aqueous solution and human saliva (2 mL/2 mL, *v*/v) were mixed under low temperature environment. And then the mixture was centrifuged at 8000 rpm for 10 min to collect the supernatant, which was further saved at −20 °C.

Human serum (1.5 mL) was added into a mixture solution of 0.2% TFA aqueous solution and 37% hydrochloric acid (0.1 mL/0.1 mL, *v*/v), and then the supernatant was collected by centrifuged at 3000 rpm for 7 min. Next, the collected supernatant (1.5 mL) was further diluted with deionized water (3 mL) and then saved at −20 °C.

Results and discussion

Synthesis of magG@PDA@Ni-MOF@Fe-MOF

The synthesis strategy of magG@PDA@Ni-MOF@Fe-MOF was illustrated in Scheme 1. Firstly, magG sheets were prepared through hydrothermal reaction. Next, dopamine was grafted onto magG sheets to form a PDA layer, increasing the hydrophilicity of material. Then, Ni-MOF, which utilized 1,4-BDC as chelating agent, was successfully functionalized on the PDA layer to form magG@PDA@Ni-MOF. Finally, Fe-MOF was functionalized on Ni-MOF in similar manner to obtain magG@PDA@Ni-MOF@Fe-MOF. What worth mentioning was that MOFs formed a shell outside the PDA.

Choice of materials

Based on the large specific surface of graphene, a considerable quantity of functionalized substances can be grafted on the surface. The introduction of magnetism allowed the material to be separated from the solution quickly. The modification of PDA improves the hydrophilicity of material, while PDA also provided a rich binding sites for the chelation of metal ions. MOFs not only provided a large amount of active metal centers to capture phosphopeptides, but also endowed the material with the ability of fast mass transfer. Because of the enrichment preference of different metal ions were not same, such as Ti(IV) tended to enrich monophosphopeptides while Ga(III) tended to enrich multi-phosphopeptides, the combination of metal ions with different enrichment preference results in complementary enrichment and obtain several times phosphoproteomic coverage. Thus, the selection of Fe-MOF biased to monophosphopeptides and Ni-MOF biased to multiple-phosphopeptides achieves the goal of global phosphopeptides enrichment and obtain excellent effect. It's foreseeable that such binary magnetic MOFs material, with a large specific surface area, good magnetic and hydrophilic properties, fast mass transfer, and active metal centers, have broad potential in phosphopeptidomics research.

Characterization

The morphology of synthetic magG@PDA@Ni-MOF@Fe-MOF was gained through scanning electron microscope (SEM), and transmission electron microscope (TEM). From SEM image of magG@PDA@Ni-MOF@Fe-MOF (Fig. 1a), magnetic balls were uniformly distributed on the surface of graphene, and the surface of Fe_3O_4 and graphene became rough after modified with MOFs, revealing MOFs were grafted on PDA layer. TEM image of magG@PDA@Ni-MOF@Fe-MOF (Fig. 1b) also manifested the successfully formation of the MOFs layer. Then it was randomly selected 20 magnetic balls to calculate the size distribution of the nanospheres. And the size distribution of the nanospheres was a

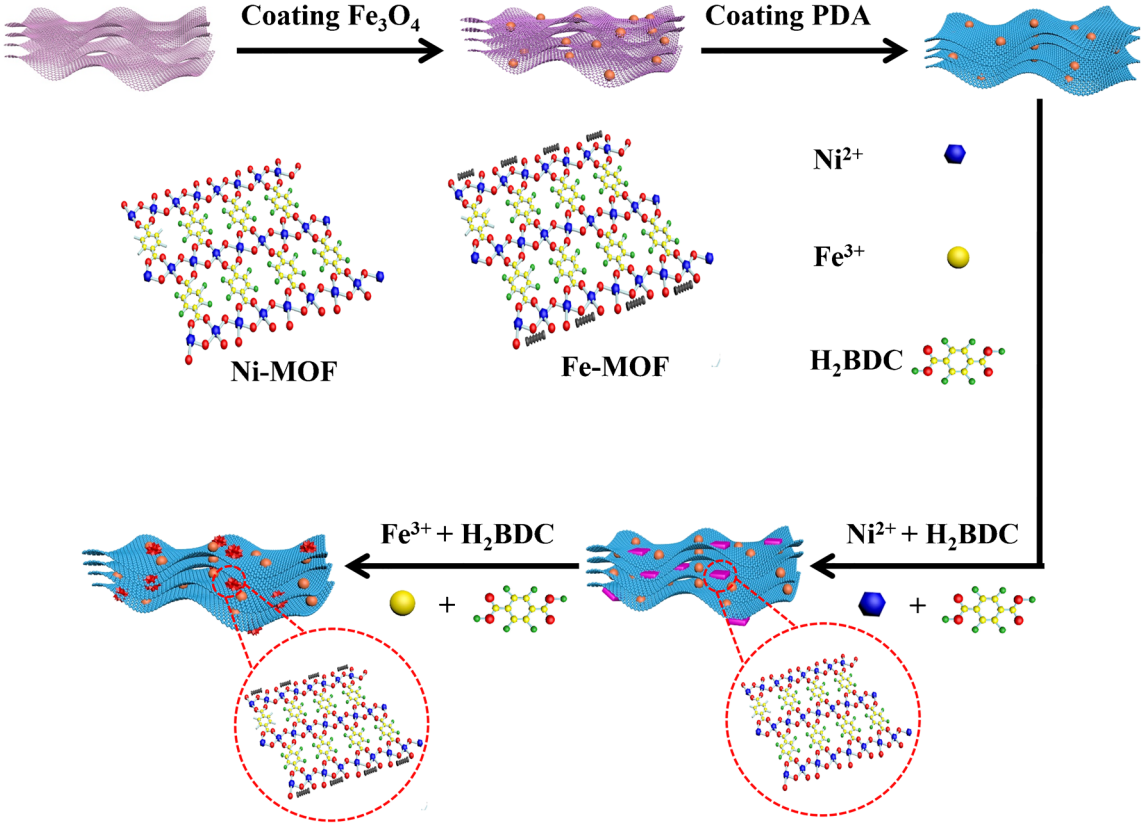

Scheme 1 The synthetic strategy of magG@PDA@Ni-MOF@Fe-MOF

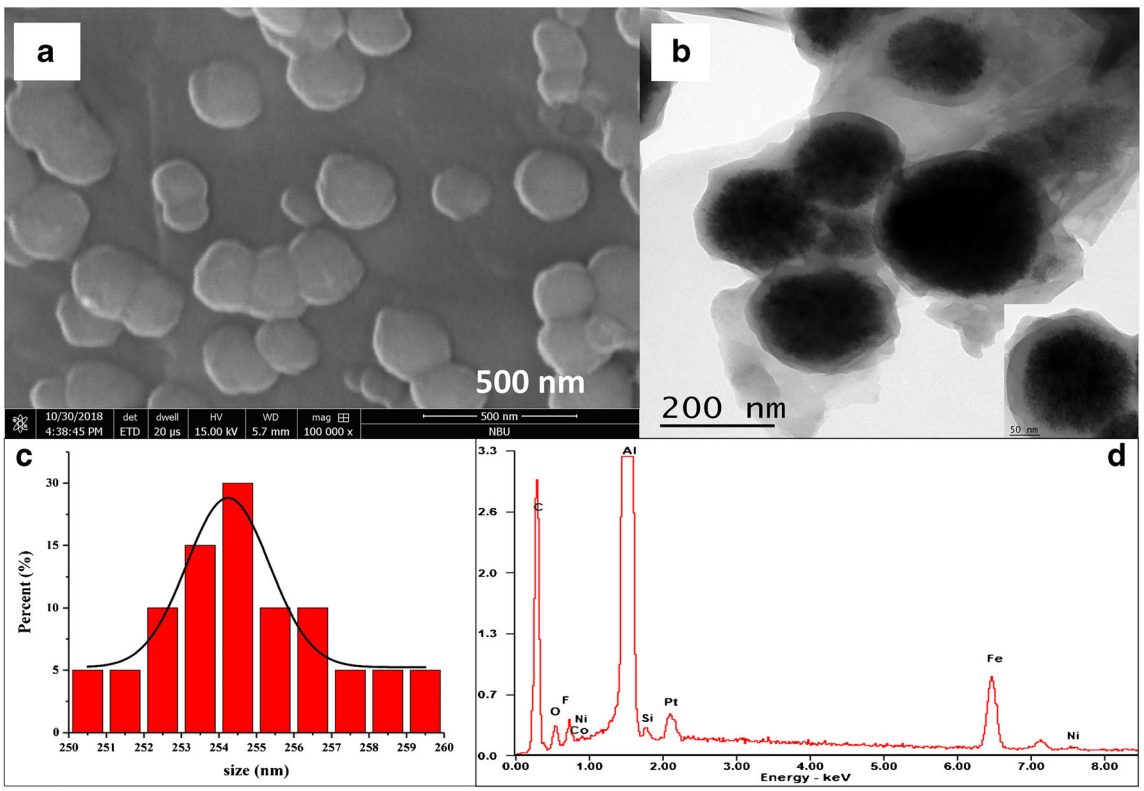

Fig. 1 **a** SEM image of magG@PDA@Ni-MOF@Fe-MOF; **b** TEM image of magG@PDA@Ni-MOF@Fe-MOF; **c** the histograms of the size distribution of magG@PDA@Ni-MOF@Fe-MOF; **d** Energy dispersive X-ray (EDX) spectrum data of magG@PDA@Ni-MOF@Fe-MOF

range from 251.9 to 259.2 nm with an average size of 254.7 ± 2.1 nm (Fig. 1c). EDX analysis (Fig. 1d) verified the presence of nickel element and iron element.

The FT-IR spectra of magG, magG@PDA, magG@PDA@Ni-MOF, and magG@PDA@Ni-MOF@Fe-MOF were shown in Fig. S1. The adsorption vibration of 1620 cm^{-1} attributed to C=N vibration, proved the PDA layer had modified on magG sheets. Besides, the band at 465 cm^{-1}, 1397 cm^{-1} and 665 cm^{-1} were belong to the vibration of Ni-O, C=C and = C-H, respectively, which demonstrated MOFs were certainly grafted on PDA layer. Moreover, the movement of zeta potential (Fig. S2) further indicated the material was synthesized step by step.

Thermogravimetric analysis (TGA) results were manifested the thermal stability and mass ratios of components of material (Fig. S3). At approximately 670 °C, the weight loss of 11% was from the formed PDA layer, which indicated an excellent thermal stability under 650 °C. At approximately 530 °C, a mass loss of 16% was observed after modified with Ni-MOF, revealing the successfully formed the MOF shell outside the PDA. After further modification of Fe-MOF, the weight loss added another 2%, which was the evidence that the modification of Fe-MOF. More worth mentioning was the superior thermal stability of MOFs under 500 °C.

Investigation of Phosphopeptides enrichment by magG@PDA@Ni-MOF@Fe-MOF

To test the selectivity of composite material, it was used magG@PDA@Ni-MOF@Fe-MOF to isolate the phosphopeptides which was in tryptic digested of β-casein. The enrichment experiment of phosphopeptides was illustrated in Scheme 2. For comparison, two composite materials (magG@PDA@Ni-MOF and magG@PDA@Fe-MOF) were investigated the enrichment ability by the same experiment as well. Before enrichment, nonphosphopeptides held the main peaks of spectrum when the consistency of β-casein digests was 400 fmol (Fig. 2a). After enrichment with magG@PDA@Ni-MOF, multiple-phosphopeptides behaved strong signals while monophosphopeptides held only weak signals (Fig. 2c), which was highlighted by the signals at m/z 2061 and m/z 3122. And when used magG@PDA@Fe-MOF (Fig. 2d) to enrich, the result was in contrast. Not only the intensities of multiple-phosphopeptides were greatly lessened, but also the kinds were decreased, which indicated Ni(II) was biased towards multiple-phosphopeptides while Fe(III) tended to enrich monophosphopeptides. The detailed information can be found in Table S1 of the Electronic Supporting Information.

After enrichment with magG@PDA@Ni-MOF@Fe-MOF, it was detected two monophosphopeptides, four multiple-phosphopeptides and two dephosphorylated fragments, including all phosphopeptides which were enriched by magG@PDA@Ni-MOF and magG@PDA@Fe-MOF. And from Fig. 2b, not only the signals at m/z 2061 and m/z 3122 were the average result of the two single metal functionalized materials (magG@PDA@Ni-MOF and magG@PDA@Fe-MOF) as expected, but also the intensity at m/z 2556 was surprisingly well above average. Besides, although monophosphopeptides dominated the spectrum, there were still arose many multiphosphopeptides with not low in intensity. We attributed the greatly enhanced enrichment efficiency to the uniform distribution of Ni(II) and Fe(III) so to achieve the complementary results. Moreover, the excellent selectivity for phosphopeptides was known from clear background and almost no presence of nonphosphopeptides signals.

It's investigated the detection limit of magG@PDA@Ni-MOF@Fe-MOF through loading different concentrations of phosphopeptides. When the concentration was diluted to 400

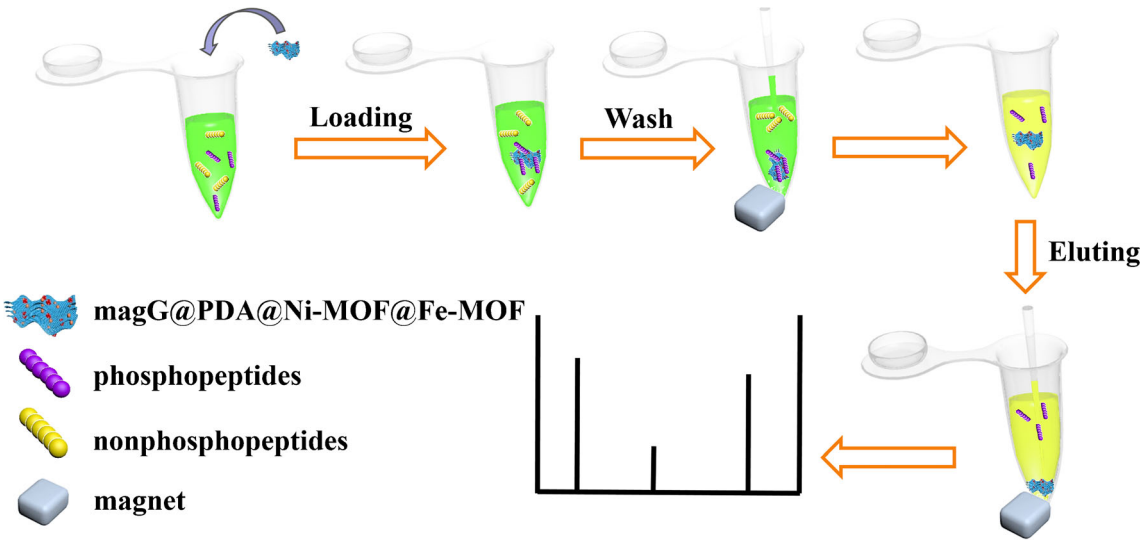

Scheme 2 Workflow of phosphopeptides enrichment by magG@PDA@Ni-MOF@Fe-MOF

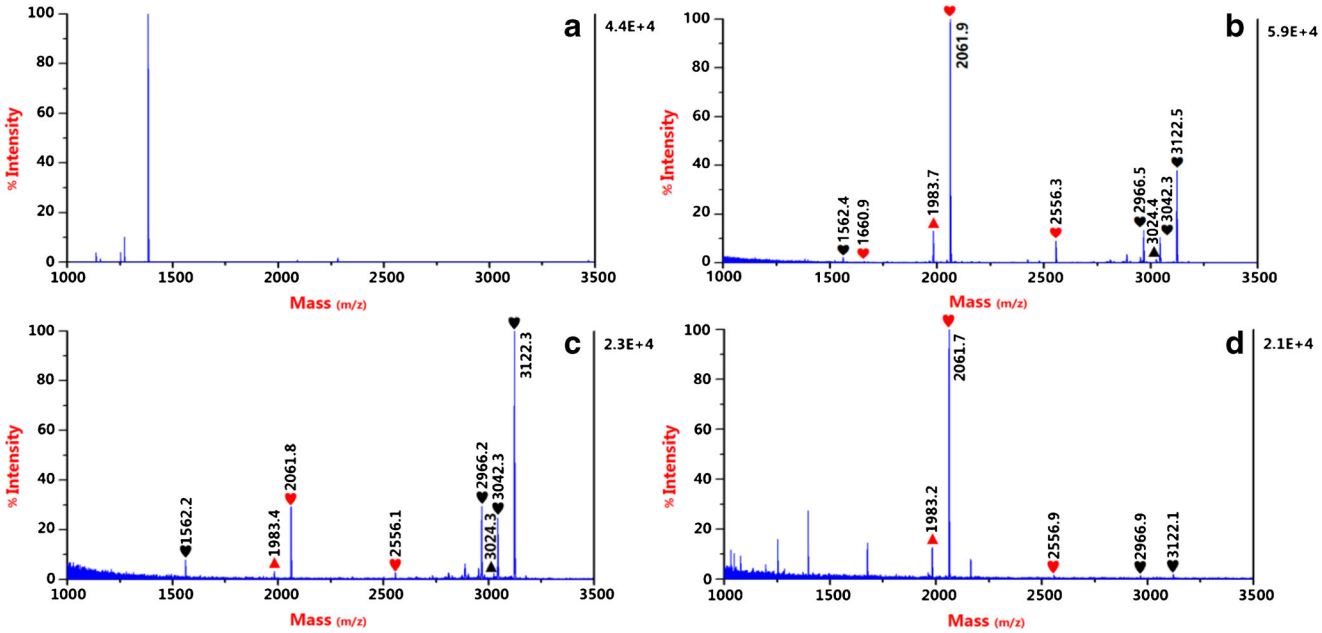

Fig. 2 MALDI-TOF mass spectra of tryptic digested β-casein (400 fmol) enriched with different materials: **a** before enrichment, **b** after treatment with magG@PDA@Ni-MOF@Fe-MOF, **c** after treatment with magG@PDA@Ni-MOF, **d** after treatment with magG@PDA@Fe-MOF, where ♥ manifests monophosphopeptide and ▲ manifests dephosphorylated fragment, ♥ manifests multiphosphopeptide and ▲ manifests dephosphorylated fragment. The experiment was performed three times under the same process ($n = 3$)

fmol (Fig. 3a), all phosphopeptides can been easily enriched by magG@PDA@Ni-MOF@Fe-MOF. Next, further diluted the density to 40 fmol (Fig. 3b), almost all multiple-phosphopeptides and monophosphopeptides were detected. And when the concentration was as low as 4 fmol (Fig. 3c), it can be still observed three peaks of phosphopeptides and dephosphorylated fragments and almost no presence of nonphosphopeptides, which declared the high sensitivity of magG@PDA@Ni-MOF@Fe-MOF. However, for magG@PDA@Ni-MOF and magG@PDA@Fe-MOF, only when the density was diluted to 40 fmol (Fig. 3d and e), the signals of phosphopeptides occupy the dominant position, which manifested the rather excellent enrichment ability of magG@PDA@Ni-MOF@Fe-MOF.

The selectivity of magG@PDA@Ni-MOF@Fe-MOF was investigated through enriching phosphopeptides in a mixture of different molar ratios of tryptic digested of β-casein and BSA. When the mixing ratio of β-casein to BSA was 1:1 (Fig. S4a), six phosphopeptides and dephosphorylated fragments were visible, which was similar to the result that in the absence of BSA interference. The above phenomenon show that magG@PDA@Ni-MOF@Fe-MOF can selectively capture phosphopeptides from the semi-complex sample solution, and non-phosphopeptides were washed away with the aid of a magnet. When the molar ratio was increased to 1:1000 (Fig. S4d), phosphopeptides still dominated the spectrum despite there were some non-phosphopeptides signals. For comparison, same process was performed with magG@PDA@Ni-MOF and magG@PDA@Fe-MOF. The outcome showed the selectivity of magG@PDA@Ni-MOF and magG@PDA@Fe-MOF was greatly reduced (Fig. S4e and S4f), which further revealed magG@PDA@Ni-MOF@Fe-MOF has good selectivity and a well potentiality to enrich phosphopeptides from complex biological sample.

Based on the micropore characteristics of MOFs and the strong force of IMAC for phosphopeptides, it was probed the rapidly enrichment ability of magG@PDA@Ni-MOF@Fe-MOF by means of altering adsorption and desorption time. When the adsorption and desorption time all were 10 s (Fig. 4a), although there only two phosphopeptides and dephosphorylated fragments were appeared, phosphopeptides dominated this very clean spectrum. Under the condition that kept desorption time changeless but altered adsorption time to 1 min (Fig. 4b), two additional phosphopeptides and dephosphorylated fragments were appeared, which demonstrated despite only prolonged a little adsorption time, the enrichment efficiency was greatly improved. Afterwards, if desorption time altered to 1 min and adsorption time became constant, the obtained spectrum (Fig. 4c) was similar to Fig. 4b except that it's cleaner. Next, when desorption time was prolonged to 15 min, the gained spectrum (Fig. 4d) were basically similar to the spectrum which was adsorption for 30 min, manifesting a large amount of phosphopeptides to be adsorbed with magG@PDA@Ni-MOF@Fe-MOF in 1 min. Exemplified with m/z 3122 to resolve the reason why multiphosphopeptides are eluted when desorption time reached to 15 min, m/z 3122

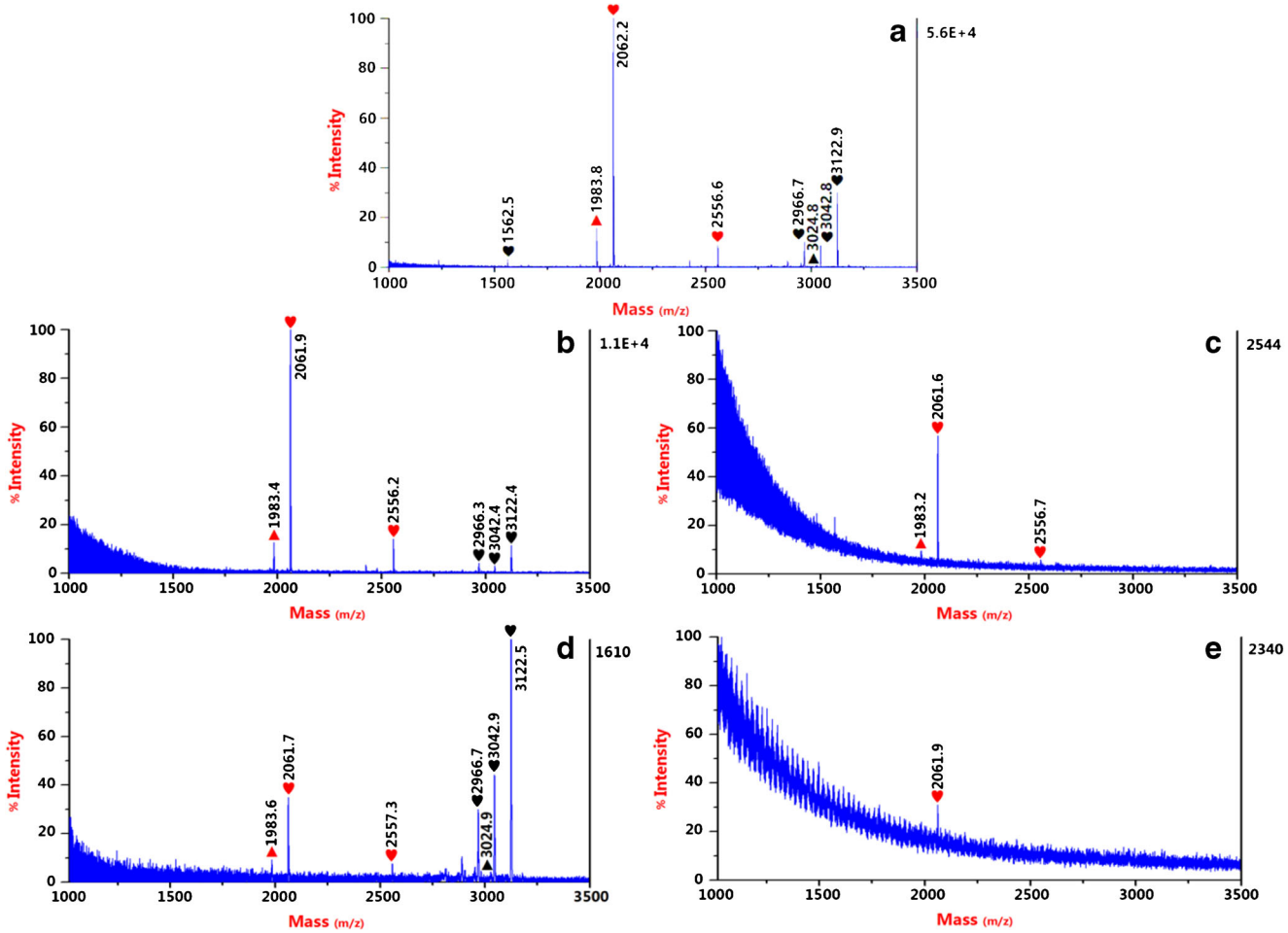

Fig. 3 MALDI-TOF mass spectra of enrichment of tryptic digested β-casein at different concentrations: **a** 400 fmol enriched by magG@PDA@Ni-MOF@Fe-MOF, **b** 40 fmol enriched by magG@PDA@Ni-MOF@Fe-MOF, **c** 4 fmol enriched by magG@PDA@Ni-MOF@Fe-MOF, **d** 40 fmol enriched by magG@PDA@Ni-MOF, **e** 40 fmol enriched by magG@PDA@Fe-MOF, where ♥ manifests monophosphopeptide and ▲ manifests dephosphorylated fragment, ♥ manifests multiphosphopeptide and ▲ manifests dephosphorylated fragment. The experiment was performed three times under the same process ($n = 3$)

had four phosphorylation sites. The above results manifested that magG@PDA@Ni-MOF@Fe-MOF had a strong ability to rapidly enrichment (1 min).

In addition, the recyclability of magG@PDA@Ni-MOF@Fe-MOF was evaluated by enrichment of tryptic digested of β-casein. Repeated experiments were executed a total of five times, and before each cycles, the used material was washed with loading buffer and ammonia aqueous solution (0.4 M) to remove the residues. Compared with the first cycle, even after five cycles, it was still observed that all phosphopeptides were captured and the strength was almost no loss. Thus the fifth mass spectrum (Fig. S5b) was almost the same as the first time (Fig. S5a), which demonstrated the unchanged ability of magG@PDA@Ni-MOF@Fe-MOF toward phosphopeptides. So one can say the prepared material had fine reusability (five cycles). Besides, three independent batches of materials were prepared according to the same preparation method and were applied in capturing phosphopeptides. As shown in the three mass spectra of Fig. S6, the intensities and types of captured phosphopeptides were very similar. And although used different batches of materials to enrich, it still achieves the goal of global phosphopeptides enrichment. All of the above indicate that the material had good reproducibility.

Select Phosphopeptides from biological samples

Human saliva, contained many low-abundance endogenous phosphopeptides, is an easily available clinical specimen, and it was used to evaluate the ability of magG@PDA@Ni-MOF@Fe-MOF to selectively enrich phosphopeptides from biological samples. Before enrichment, the main peaks of spectrum (Fig. 5a) did nonphosphopeptides held in human saliva. After enrichment by magG@PDA@Ni-MOF@Fe-MOF, 24 peaks of phosphopeptides were appeared (Fig. 5b), while nonphosphopeptides were almost not exist, and the details of phosphopeptides were listed in Table S2 and S3 of Electronic Supporting Information. Compared with the former

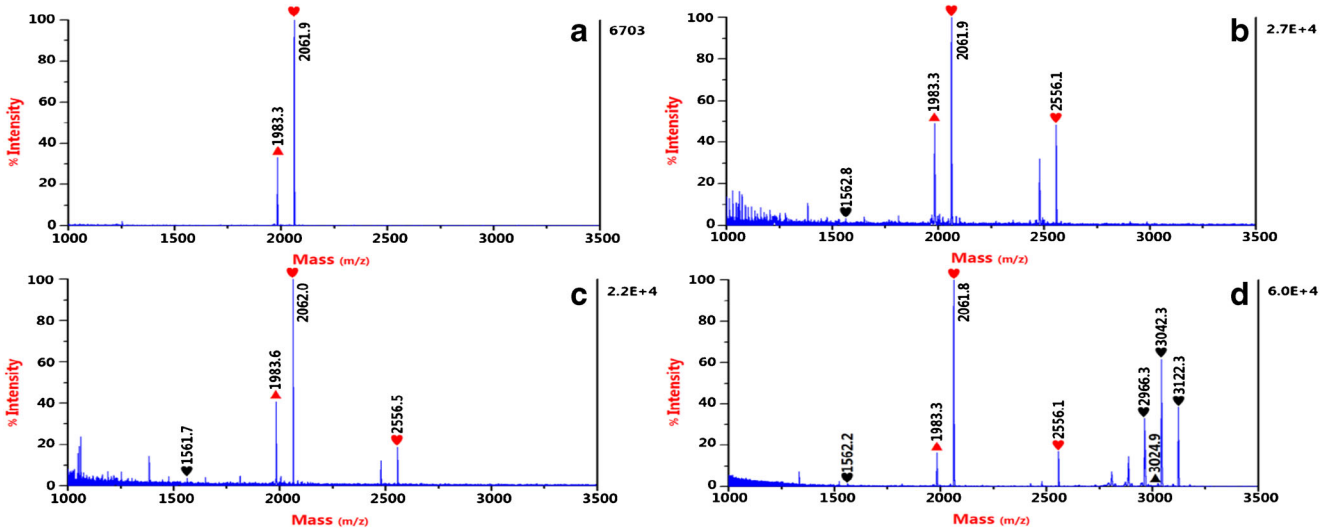

Fig. 4 MALDI-TOF mass spectra of different adsorption and desorption time to enrich tryptic digested β-casein (400 fmol): **a** adsorption and desorption time all were 10 s, **b** adsorption time was 1 min when desorption time was 10 s, **c** adsorption and desorption time all were 1 min, **d** adsorption time was 1 min when desorption time was 15 min, where ♥ manifests monophosphopeptide and ▲ manifests dephosphorylated fragment, ♥ manifests multiphosphopeptide and ▲ manifests dephosphorylated fragment. The experiment was performed three times under the same process ($n = 3$)

reports that only enriched 14 kinds of phosphopeptides [35], it can obviously know that magG@PDA@Ni-MOF@Fe-MOF has excellent performance in the selective enrichment of phosphopeptides from biological samples.

When a similar research was conducted in human serum (Fig. S7), four phosphopeptides were enriched by magG@PDA@Ni-MOF@Fe-MOF, which was consistent with former research, and the details of phosphopeptides were listed in Table S4 of Electronic Supporting Information. These results indicated a great application prospect did magG@PDA@Ni-MOF@Fe-MOF behaved in selective enrichment of phosphopeptides from complex biological samples.

A comparison between recently reported nanomaterial-based methods and our work were listed in Table 1. The above

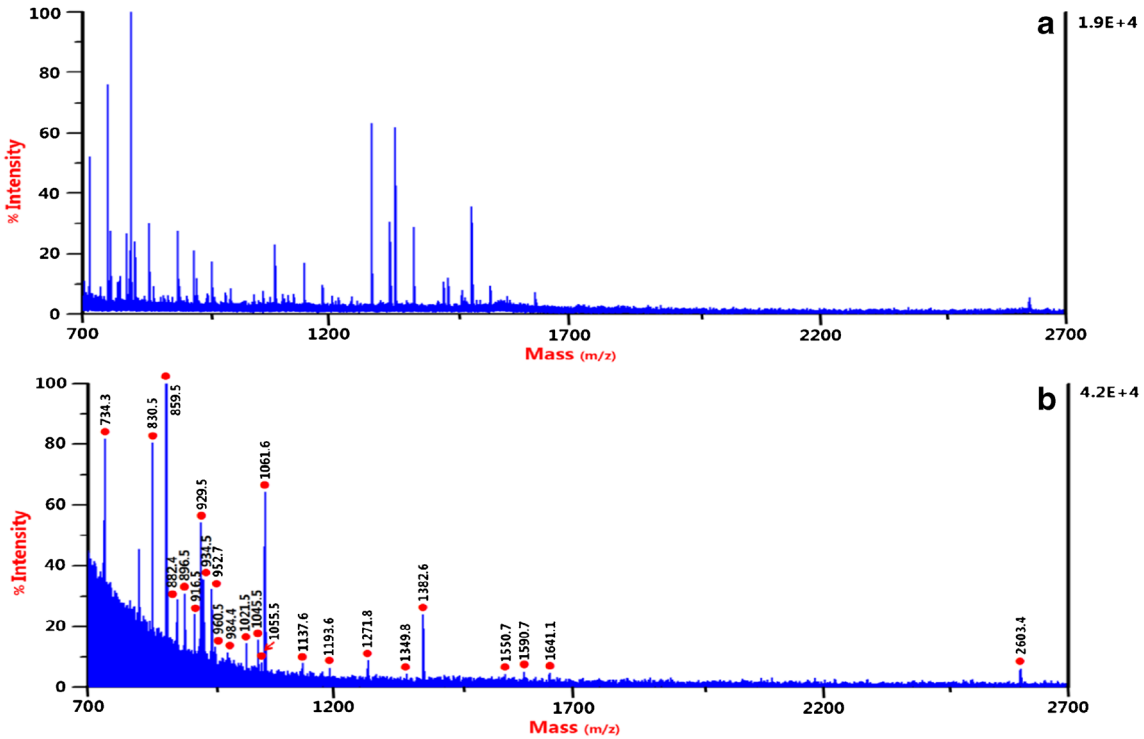

Fig. 5 MALDI-TOF mass spectra of phosphopeptides from human saliva: **a** before enrichment, **b** enrichment by magG@PDA@Ni-MOF@Fe-MOF, where ● manifests monophosphopeptide and multiphosphopeptide. The experiment was performed three times under the same process ($n = 3$)

Table 1 An overview on recently reported nanomaterial-based methods for enrichment of phosphopeptides

Materials used	Method applied	LODs	Specificity	sample	Number of endogenous peptides	Ref.
Fe_3O_4@mSiO_2-Ti^{4+}	IMAC	20 fmol	BSA:α-casein:β–casein = 500:500:1	human serum and saliva	4 and 13	[10]
Phosphate-imprinted MSNs	molecular imprinting technology	–	BSA:β-casein = 100:1	nonfat milk digests	7	[11]
SPMA	amino functionalization	10fmol	BSA:β-casein = 1000:1	non-fat milk digest and digest of rat brain lysate	19 and 1659	[13]
HOMMS@TiO_2	MOAC	8 fmol	BSA:β-casein = 1000:1	human serum	4	[14]
MG@mSiO_2-ATP-Ti^{4+}	IMAC	4 fmol	BSA:β-casein = 1000:1	human serum and saliva	4 and 19	[15]
DZMOF	IMAC	10 fmol	BSA:β-casein = 5000:1	human saliva	19	[20]
2-D Hf-BTB	IMAC	4×10^{-10} M	BSA:β-casein = 1000:1	human serum and saliva	4 and 12	[21]
Ti^{4+}-MGMSs	IMAC	0.5 fmol/μL	BSA:β-casein = 500:1	human serum and saliva	4 and 14	[35]
MagG@PDA@Ni-MOF@Fe-MOF	IMAC	4 fmol	BSA:β-casein = 1000:1	human serum and saliva	4 and 24	this work

"–" stands for not mentioned

outcome manifested that due to the complementary effects of Ni(II) and Fe(III), magG@PDA@Ni-MOF@Fe-MOF had an excellent enrichment effect on both multiphosphopeptides and monophosphopeptides, and had a highly sensitivity (4 fmol) and phosphopeptide selectivity (1:1000). Based on the microporous property of MOFs, magG@PDA@Ni-MOF@Fe-MOF also had an excellent performance for rapid enrichment (1 min). Moreover, magG@PDA@Ni-MOF@Fe-MOF had acquired approving effect in selectively capture phosphopeptides in complex biological samples, which represented magG@PDA@Ni-MOF@Fe-MOF had an extensive prospect in phosphopeptidomics analysis. However, organic solvent was used in the preparation process. Although the amount of the organic solvent used was small, the use of an environmentally friendly system such as water would be preferred.

Conclusions

In summary, binary metal ion functionalized material (magG@PDA@Ni-MOF@Fe-MOF) was synthesized with an ordinary method of ultrasonication at room temperature, which was further used for selective enrichment of phosphopeptides. Compared to single metal ion functionalized materials (magG@PDA@Ni-MOF and magG@PDA@Fe-MOF), magG@PDA@Ni-MOF@Fe-MOF has a better enrichment efficiency, higher sensitivity (4 fmol) and phosphopeptide selectivity (1:1000), and offers new thought about combining vary metal ions to reach the aim of complementary enrichment for multiphosphopeptides and monophosphopeptides. In addition, not only a fine reusability (five cycles) does magG@PDA@Ni-MOF@Fe-MOF has, but also has the ability to be rapidly enriched (1 min) which was attributed to the characteristic of the pores. When applied in complex biological samples like human saliva and human serum, magG@PDA@Ni-MOF@Fe-MOF is able to identify and condense phosphopeptides, this manifesting an extensive prospect in phosphopeptidomics .

Acknowledgements This work is supported by Zhejiang Natural Science Foundation (LQ19C050002), Ningbo Natural Science Foundation (2018A610279), and the K. C. Wong Magna Fund in Ningbo University.

Compliance with ethical standards

Conflict of interest The author(s) declare that they have no competing interests.

References

1. Peng JX, Niu H, Zhang HY, Yao YT, Zhao XY, Zhou XY, Wan LH, Kang XH, Wu RA (2018) Highly specific enrichment of multiphosphopeptides by the diphosphorylated fructose-modified dual-metal-centered zirconium-organic framework. ACS Appl Mater Interfaces 10(38):32613–32621
2. Zhao M, Xie YQ, Deng CH, Zhang XM (2014) Recent advances in the application of core-shell structured magnetic materials for the separation and enrichment of proteins and peptides. J Chromatogr A 1357:182–193
3. Zhou JQ, Liang YL, He XM, Chen LX, Zhang YK (2017) Dual-functionalized magnetic metal-organic framework for highly specific enrichment of phosphopeptides. ACS Sustain Chem Eng 5(12):11413–11421

4. Lundby A, Secher A, Lage K, Nordsborg NB, Dmytriyev A, Lundby C, Olsen JV (2012) Quantitative maps of protein phosphorylation sites across 14 different rat organs and tissues. Nat Commun 3:876
5. Xu HM, Liu M, Huang XD, Min QH, Zhu JJ (2018) Multiplexed quantitative MALDI MS approach for assessing activity and inhibition of protein kinases based on postenrichment dephosphorylation of phosphopeptides by metal-organic framework-templated porous CeO_2. Anal Chem 90(16):9859–9867
6. Chen YJ, Xiong ZC, Peng L, Gan YY, Zhao YM, Shen J, Qian JH, Zhang LY, Zhang WB (2015) Facile preparation of core-shell magnetic metal-organic framework nanoparticles for the selective capture of phosphopeptides. ACS Appl Mater Interfaces 7(30):16338–16347
7. Yang SS, Chang YJ, Zhang H, Yu XZ, Shang WB, Chen GQ, Chen DDY, Gu ZY (2018) Enrichment of phosphorylated peptides with metal-organic framework nanosheets for serum profiling of diabetes and phosphoproteomics analysis. Anal Chem 90(22):13796–13805
8. Steen H, Jebanathirajah JA, Rush J, Morrice N, Kirschner MW (2006) Phosphorylation analysis by mass spectrometry: myths, facts, and the consequences for qualitative and quantitative measurements. Mol Cell Proteomics 5(1):172–181
9. Gao CH, Lin G, Lei ZX, Zheng Q, Lin JS, Lin Z (2017) Facile synthesis of core-shell structured magnetic covalent organic framework composite nanospheres for selective enrichment of peptides with simultaneous exclusion of proteins. J Mater Chem B 5(36):7496–7503
10. Yao JZ, Sun NR, Wang JW, Xie YQ, Deng CH, Zhang XM (2017) Rapid synthesis of titanium(IV)-immobilized magnetic mesoporous silica nanoparticles for endogenous phosphopeptides enrichment. Proteomics 17(8):1600320
11. Chen Y, Li DJ, Bie ZJ, He XP, Liu Z (2016) Coupling of phosphate-imprinted mesoporous silica nanoparticles-based selective enrichment with matrix-assisted laser desorption ionization-time-of-flight mass spectrometry for highly efficient analysis of protein phosphorylation. Anal Chem 88(2):1447–1454
12. Chen CT, Wang LY, Ho YP (2011) Use of polyethylenimine-modified magnetic nanoparticles for highly specific enrichment of phosphopeptides for mass spectrometric analysis. Anal Bioanal Chem 399(8):2795–2806
13. Luo B, Yang MG, Jiang PP, Lan F, Wu Y (2016) Multi-affinity sites of magnetic guanidyl-functionalized metal-organic framework nanospheres for efficient enrichment of global phosphopeptide. Nanoscale 10(18):8391–8396
14. Yan YH, Zhang XG, Deng CH (2014) Designed synthesis of titania nanoparticles coated hierarchially ordered macro/mesoporous silica for selective enrichment of phosphopeptides. ACS Appl Mater Interfaces 6(8):5467–5471
15. Su J, He XW, Chen LX, Zhan YK (2017) Adenosine phosphate functionalized magnetic mesoporous graphene oxide nanocomposite for highly selective enrichment of phosphopeptides. ACS Sustain Chem Eng 6(2):2188–2196
16. Salimi K, Kip C, Celikbicak O, Usta DD, Pinar A, Salih B, Tuncel A (2019) Ti(IV) attached-phosphonic acid functionalized capillary monolith as a stationary phase for in-syringe-type fast and robust enrichment of phosphopeptides. Biomed Chromatogr 33(6):e4488
17. Sun NR, Wang JW, Yao JZ, Chen HM, Deng CH (2019) Magnetite nanoparticles coated with mercaptosuccinic acid-modified mesoporous titania as a hydrophilic sorbent for glycopeptides and phosphopeptides prior to their quantitation by LC-MS/MS. Microchim Acta 186(3)
18. Zhang KN, Hu DH, Deng SM, Han M, Wang XF, Liu HL, Liu Y, Xie MX (2019) Phytic acid functionalized Fe_3O_4 nanoparticles loaded with Ti(IV) ions for phosphopeptide enrichment in mass spectrometric analysis. Microchim Acta 186(2):68
19. Wang JW, Wang ZD, Sun NR, Deng CH (2019) Immobilization of titanium dioxide/ions on magnetic microspheres for enhanced recognition and extraction of mono- and multi-phosphopeptides. Microchim Acta 186(4)
20. Peng JX, Zhang HY, Li X, Liu SJ, Zha XY, Wu J, Kang XH, Qin HQ, Pan ZF, Wu RA (2016) Dual-metal centered zirconium-organic framework: a metal-affinity probe for highly specific interaction with phosphopeptides. ACS Appl Mater Interfaces 8(51):35012–35020
21. Xiao J, Yang SS, Wu JX, Wang H, Yu XZ, Shang WB, Chen GQ, Gu ZY (2019) Highly selective capture of monophosphopeptides by two-dimensional metal-organic framework nanosheets. Anal Chem 91(14):9093–9101
22. Maka VK, Mukhopadhyay A, Savitha G, Moorthy JN (2018) Fluorescent 2D metal-organic framework nanosheets (MONs): design, synthesis and sensing of explosive nitroaromatic compounds (NACs). Nanoscale 10(47):22389–22399
23. Van de Voorde B, Ameloot R, Stassen I, Everaert M, De Vos D, Tan JC (2013) Mechanical properties of electrochemically synthesised metal-organic framework thin films. J Mater Chem C 1(46):7716–7724
24. Jiang M, Li J, Cai XF, Zhao Y, Pan LJ, Cao QQ, Wang DH, Du YW (2018) Ultrafine bimetallic phosphide nanoparticles embedded in carbon nanosheets: two-dimensional metal-organic framework-derived non-noble electrocatalysts for the highly efficient oxygen evolution reaction. Nanoscale 10(42):19774–19780
25. Wen LL, Zhou L, Zhang BG, Meng XG, Qu H, Li DF (2012) Multifunctional amino-decorated metal-organic frameworks: nonlinear-optic, ferroelectric, fluorescence sensing and photocatalytic properties. J Mater Chem 22(42):22603–22609
26. Dmello ME, Sundaram NG, Singh A, Singh AK, Kalidindi SB (2019) An amine functionalized zirconium metal-organic framework as an effective chemiresistive sensor for acidic gases. Chem Commun 55(3):349–352
27. Huan WW, Xing MY, Cheng C, Li J (2018) Facile fabrication of magnetic metal-organic framework nanofibers for specific capture of phosphorylated peptides. ACS Sustain Chem Eng 7(2):2245–2254
28. Jiang JB, Sun XN, She XJ, Li JJ, Li Y, Deng CH, Duan GL (2018) Magnetic microspheres modified with Ti(IV) and Nb(V) for enrichment of phosphopeptides. Microchim Acta 185(6):309
29. Liu QJ, Sun NR, Gao MX, Deng CH (2018) Magnetic binary metal-organic framework as a novel affinity probe for highly selective capture of endogenous phosphopeptides. ACS Sustain Chem Eng 6(3):4382–4389
30. Rui K, Zhao GQ, Chen YP, Lin Y, Zhou Q, Chen JY, Zhu JX, Sun WP, Huang W, Dou SX (2018) Hybrid 2D dual-metal-organic frameworks for enhanced water oxidation catalysis. Adv Funct Mater 28(26):1801554
31. Zeng J, Ji XX, Ma YH, Zhang ZX, Wang SG, Ren ZH, Zhi CY, Yu J (2018) 3D graphene fibers grown by thermal chemical vapor deposition. Adv Mater 30(12):1705380
32. Fei HL, Dong JC, Wan CZ, Zhao ZP, Xu X, Lin ZY, Wang YL, Liu HT, Zang KT, Luo J, Zhao SL, Hu W, Yan WS, Shakir I, Huang Y, Duan XF (2018) Microwave-assisted rapid synthesis of graphene-supported single atomic metals. Adv Mater 30(35):1802146
33. Wang YX, Wang SH, Niu HY, Ma YR, Zeng T, Cai YQ, Meng ZF (2013) Preparation of polydopamine coated Fe_3O_4 nanoparticles and their application for enrichment of polycyclic aromatic hydrocarbons from environmental water samples. J Chromatogr A 1283:20–26
34. Liu YL, Ai KL, Lu LH (2014) Polydopamine and its derivative materials: synthesis and promising applications in energy, environmental, and biomedical fields. Chem Rev 114(9):5057–5115
35. Sun NR, Deng CH, Li Y, Zhang XM (2014) Size-exclusive magnetic graphene/mesoporous silica composites with titanium(IV)-immobilized pore walls for selective enrichment of endogenous phosphorylated peptides. ACS Appl Mater Interfaces 6(14):11799–11804